Photogrammetry-Based Analysis of the On-orbit Structural Dynamics of the Roll-Out Solar Array

Matthew K. Chamberlain[1]
NASA Langley Research Center, Hampton VA 23681

Steven H. Kiefer[2]
Deployable Space Systems, Santa Barbara CA 93111

and

Jeremy A. Banik[3]
Air Force Research Laboratory, Space Vehicles Directorate, Kirtland AFB, NM 87117

The Roll-Out Solar Array (ROSA) flight experiment was launched to the International Space Station (ISS) on June 3rd, 2017. ROSA is an innovative, lightweight solar array with a flexible substrate that makes use of the stored strain energy in its composite structural members to provide deployment without the use of motors. This paper will discuss the results of various structural dynamics experiments conducted on the ISS during the weeks following launch. Data gathered from instrumentation on the solar array wing during the experiments was previously compared with pre-flight predictions from two different Finite Element Modeling (FEM) efforts. In this paper, data generated from photogrammetry is compared with accelerometer data and used to extend previous conclusions. Whereas previous analyses were only able to track the accelerations of six discrete points on the structure and photovoltaic (PV) blanket of ROSA, the photogrammetry analysis makes available displacements for dozens of points distributed throughout the array. This larger data set makes it possible to compare higher-order PV blanket modes with FEM predictions, in addition to verifying conclusions reached using accelerometer data. The goal in this effort was to better understand the performance of ROSA and to improve modeling efforts for future designs of similar solar arrays.

I. Introduction

COMMERCIAL and governmental activities in space demand increases in electrical power at a low mass and volume penalty. For this reason, the Air Force Research Laboratory (AFRL), the National Aeronautics and Space Administration (NASA), and Deployable Space Systems, Inc. (DSS), developed the Roll-Out Solar Array (ROSA) as a lightweight alternative to conventional rigid panel solar arrays. As is implied in its name, the key feature of ROSA is that the structure and photovoltaics are rolled up on a mandrel for launch. AFRL and the Department of Defense (DoD) Space Test Program led the development of a 5.40 meter long by 1.67 meter wide experimental ROSA wing that was launched to the International Space Station (ISS) in June of 2017. After two weeks in space, ROSA was removed from the depressurized trunk portion of the Dragon capsule using the ISS Special Purpose Dexterous Manipulator (SPDM), and positioned for deployment as seen in Fig. 1. Over the next seven days, ROSA was the subject of a series of experiments to measure its functionality in the extreme temperatures and micro-gravity of orbital flight. Following deployment on the first day of experimentation, four and a half days of structural dynamics tests were carried out, followed by tests of the performance of photovoltaics. A vast amount of data was gathered from

[1] Research Aerospace Engineer, Structural Dynamics Branch, 4B West Taylor St, AIAA Senior Member
[2] Structural Analyst, 460 Ward Dr, AIAA Member
[3] Senior Research Engineer, 3550 Aberdeen Avenue SE, AIAA Associate Fellow

these experiments, which are described along with the flight operations in Refs. [1-9]. In this work, data gathered from many of these experiments were compared with analytical predictions of deployment, forced vibration response, eclipse exit thermal-structural response, and power production. This work focuses on the structural dynamics results of the wing on-orbit, in particular the data gathered from photogrammetry, supplementing data gathered from accelerometers and analyzed in Ref. [10].

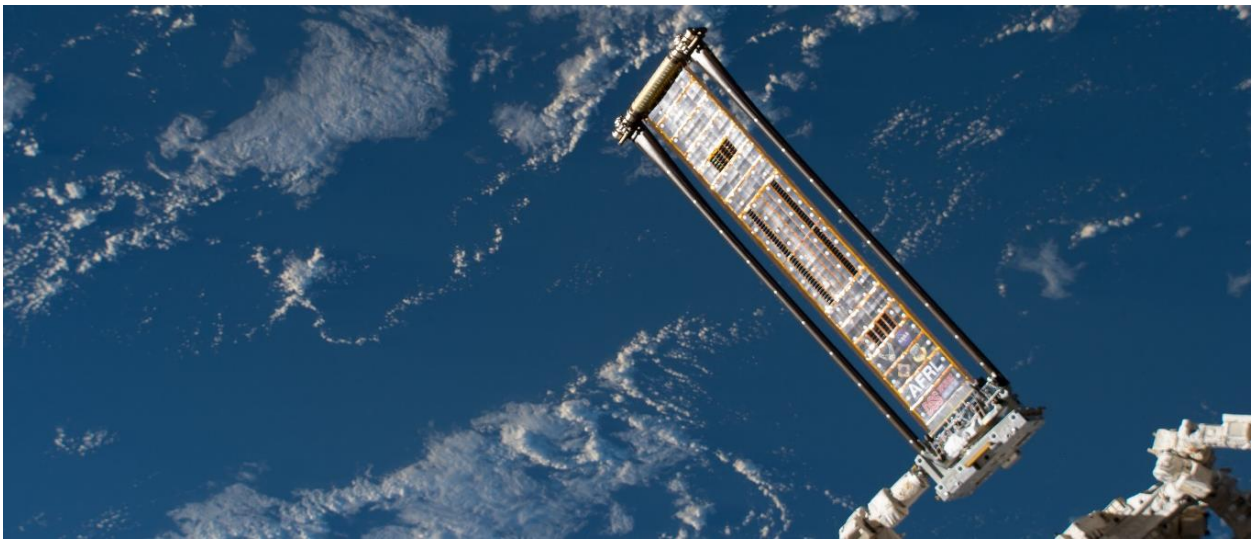

Fig. 1 ROSA flight experiment on ISS (note SPDM holding ROSA FRAM at bottom right)

ROSA consists of a pair of longitudinally-oriented high-strain-composite slit tube booms attached at their tip to a mandrel and at their root to a yoke and spacecraft adapter. The Integrated Modular Blanket Assembly (IMBA or simply the "blanket") is tensioned between the spreader bar at its root and the root tube structure. It consists of lightweight photovoltaic power modules attached to mesh. When flattened and rolled up on the mandrel to be stowed for launch as shown in Fig. 2, the composite slit tubes on ROSA store the strain energy needed for deployment. This eliminates the need for a deployment motor while reducing the part count and complexity of the overall solar array.

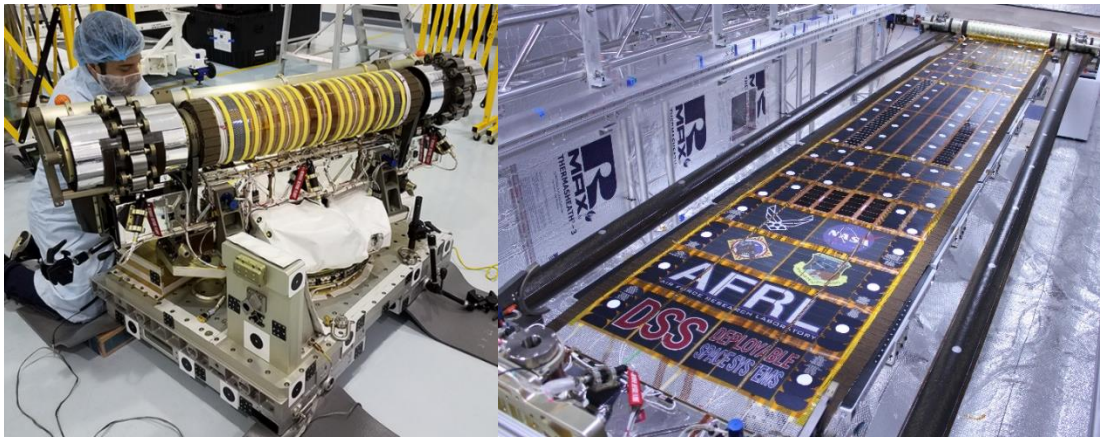

Fig. 2 Layout of the ISS ROSA flight experiment wing stowed and deployed

For the ROSA flight experiment on ISS, the standard design of the solar array wing was modified to fit inside the unpressurized trunk of the Dragon spacecraft. The IMBA was partially populated with three different types of solar cells. In addition, the composite booms remained flattened to the mandrel, even when the wing was deployed to allow retraction of the wing at the end of experimentation. The means of retraction was a dedicated motor and lanyard that are not standard elements of a ROSA since retraction is not usually desired. The root of the ROSA array was attached to a baseplate that was bolted to a Flight Releasable Attachment Mechanism (FRAM). The baseplate included a linear actuator driven by a stepper motor that provided base excitation in the out-of-plane direction during experimentation.

In previous work [10], data gathered from accelerometers on the solar array was compared with pre-flight finite element analyses. In this paper, the prior results and analyses will be compared with new data being generated from video recorded during experimentation. Of particular interest are the structural mode shapes below 2 Hz. Photogrammetry methods [11] were used to extract data that gives a far more comprehensive picture of the dynamics of the solar array. The remainder of this paper describes the instrumentation of the wing, the types of experiments that were run while the solar array wing was in space, the prior results obtained from accelerometers, and the methods used to post-process photogrammetry data. Finally, the data from photogrammetry is compared with the prior results and with finite element model (FEM) results.

II. Instrumentation, Data Collection, and Processing

During experiments, data relevant to the dynamics of the array were gathered from ROSA in two ways: from a handful of accelerometers located at a few key points, and from video of photogrammetry targets scattered extensively over the entire structure. As seen in Fig. 3, one-axis accelerometers were located at the center and both edges of the IMBA blanket at the middle of its length to capture blanket modes. Similarly, accelerometers were located at the center and ends of the mandrel in order to capture wing structure modes. Two other accelerometers were placed at the roots of the booms, providing the data sources closest to the input signal. All of the single-axis accelerometers on the array were oriented to measure out-of-plane excitation. Finally, a tri-axial accelerometer was placed on the experimental base plate below the linear actuator to monitor the state of the base of the experiment where it interfaced with the robot arm, however this accelerometer was damaged prior to flight and the data it generated is questionable. All the single axis accelerometers were oriented to measure movement out of the plane of the array.

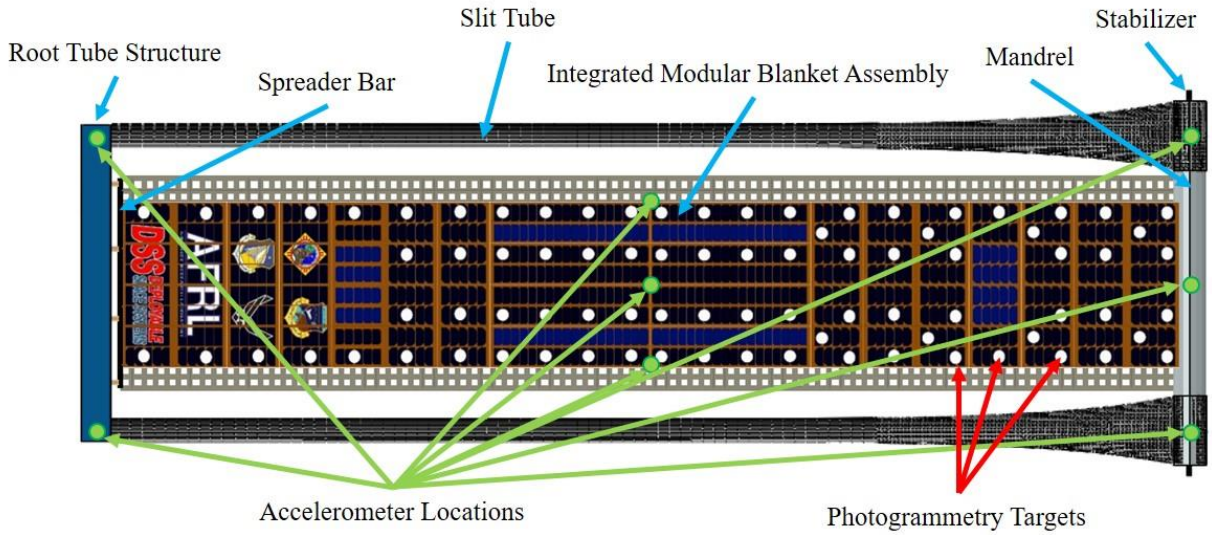

Fig. 3 Instrumentation included on deployed ROSA solar array wing

The entire solar array wing, including the booms and IMBA, was marked with reflective photogrammetry targets to enable tracking during both daylight and eclipse conditions. Some of the targets on the IMBA are shown in Fig. 3 while others were located on the opposite side of the stabilizer, along the composite slit tubes, at various points on the root structure, and on various surfaces of the FRAM. The position of the SPDM throughout the week of experimentation was chosen so that it could be viewed from the maximum number of stationary cameras located on the exterior of the space station at various distances and angles. During key experiments, video feeds from four to five views available from the ROSA and ISS cameras were recorded. These recordings were viewed in real-time but also downloaded later at full resolution for photogrammetric analysis. Further information on the methods used in planning and executing the study of ROSA dynamics using photogrammetry can be found in Ref. [11].

III. On-Orbit Experiments

The ROSA flight experiment on ISS had a number of scientific objectives, including demonstration of deployment and photovoltaic performance but the bulk of the time spent in space was used to try to characterize the structural dynamics of the solar array in microgravity under different conditions. Of particular interest was data that could be used to identify and characterize the first few bending modes of the array. Because of the nature of ROSA, it has both structural modes that one might expect from a long flat object, and distinct blanket modes due to the tensioned IMBA "blanket" held between the more rigid structure. Model predictions prior to flight suggested that several structural and blanket modes would occur below 2 Hz. These low frequency structure and blanket modes were the focus of the three sets of dynamics experiments:

- **Sine Sweeps -** In order to excite out of plane motion in the solar array structure, a linear actuator driven by a stepper motor was included in the ROSA flight experiment and located between the root of the solar array and the FRAM to which it was attached. For each experiment, the actuator was pre-programmed to apply sinusoidal motion with the desired duration, amplitude, and frequency range. After initial calibration runs that swept over wide ranges of frequencies to identify the system modes on-orbit, narrower sweeps were used to excite particular groups of modes during the daytime and at night. 97 sine sweep runs were carried out, most lasting three to five minutes.
- **Free Decay Tests** – The free decay of the wing in vacuum was tested by continuing to record data from accelerometers for up to a minute after base excitation had concluded.
- **Eclipse Entry/Exit Tests** – During a number of orbits, the accelerometers in the ROSA wing were recording data as the wing either exited eclipse and was warmed by direct sunlight, or entered darkness and rapidly cooled down. Since the slit tube booms and IMBA blanket were made with materials with low coefficients of thermal expansion (CTE), accelerometers on the mandrel and blanket recorded no significant events during eclipse entry. During eclipse exit, however, very small accelerations were seen in the blanket only [10]. These accelerations were so small that eclipse entry and exit events are not examined in this paper.

IV. Pre-Flight Modeling and Analysis

Two separate finite element analysis (FEA) efforts in Ansys and Abaqus were undertaken in an effort to predict the dynamics of ROSA. The models produced in this effort [12] were validated by comparing their predictions for the ground test version of ROSA prior to flight. Slightly different models were used to make pre-flight predictions of the on-orbit performance of ROSA. For the flight version of the wing, each model was used to predict modes as well as mode shapes as shown in Table 1 and Fig. 4. In each model, the first structural mode was an out of plane "diving board" mode in the vicinity of 0.52 Hz with the second mode having a structural twist shape and occurring around 0.65 Hz. Above those two structural modes, a large number of modes associated solely with the movement of the IMBA occur. More details on the modeling effort and post-flight model calibration will be discussed in an accompanying paper [12].

Table 1 Summary of ROSA modes and mode shapes from finite element models

Abaqus Model			ANSYS Model		
Mode	**Frequency (Hz)**	**Shape**	**Mode**	**Frequency (Hz)**	**Shape**
1	0.50	Structural Bending	1	0.54	Structural Bending
2	0.64	Structural Torsion	2	0.66	Structural Torsion
3	0.98	Blanket Drum	3	0.91	Blanket Torsion
4	1.24	Blanket Torsion	4	0.93	Blanket Saddle
5	1.88	2nd Order Blanket Drum	5	0.94	Blanket Drum
6	2.22	Lead-Lag in Plane	6	1.12	2nd Order Lateral Blanket Drum
			7	1.49	3rd Order Lateral Blanket Drum
			8	1.78	2nd Order Blanket Twist
			9	1.79	2nd Order Blanket Drum
			10	1.82	2nd Order Blanket Saddle
			11	1.87	Lead-Lag in Plane
			12	2.00	3rd Order Blanket Twist

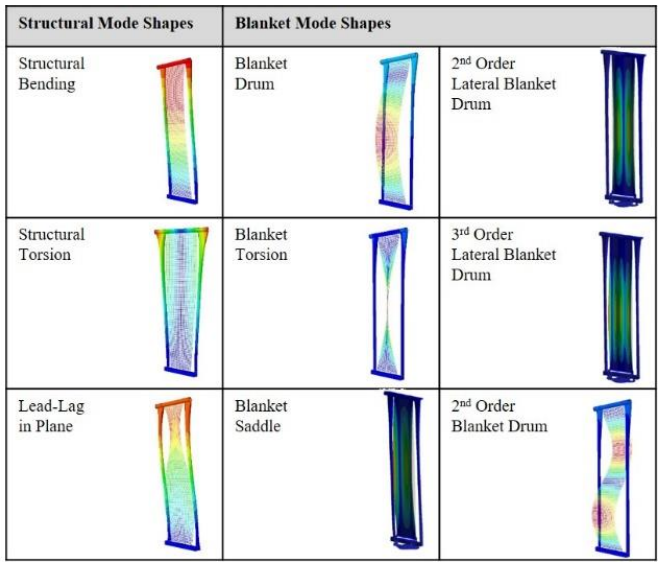

Fig. 4 Summary of ROSA FEM modes and mode shapes from both models

V. Prior Results

In previous work [10], accelerometer data was post-processed and analyzed using two methods in an attempt to identify the ROSA system natural frequencies, mode shapes, and damping. Data that was originally recorded at a rate of 200 Hz on the ISS were downlinked and filtered in various ways to help isolate system modes by identifying the peaks in the Fast Fourier Transform (FFT) of the responses. The data were also used with the Eigenvalue Realization Algorithm (ERA) [13, 14] to identify mode frequencies *and* shapes. Damping was also calculated using these two different methods. Hundreds of potential modes were identified from dozens of runs, as shown in a single plot Figure 5. After aggregating the results from dozens of experiments, eight likely modes were identified below 2 Hz, as shown in Table 2. The two methods calculated different damping values (see Table 3) but for five of the first six structural modes, the frequencies were similar.

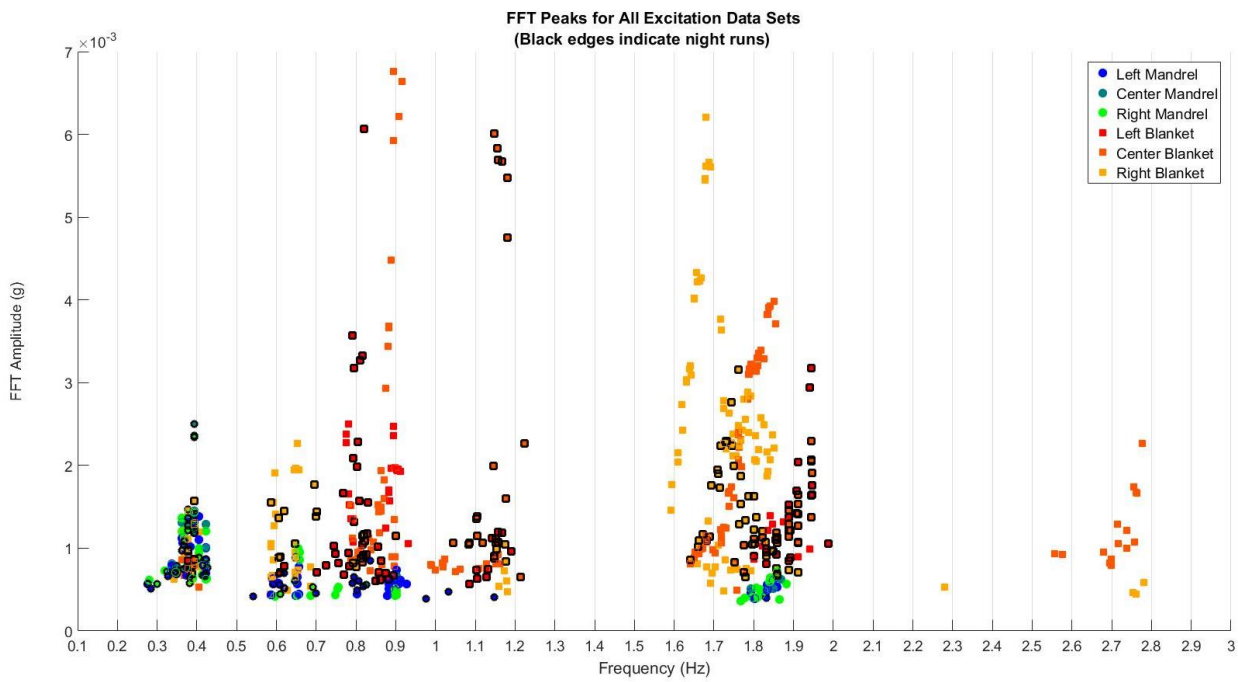

Fig. 5 FFT peaks from excitation phase of all data runs

Two unexpected phenomena were observed during this experiment. First, the fundamental system bending mode was measured to be 20% lower than predicted by finite element models. This mode also seemed highly damped and was far more difficult to excite than during pre-flight ground tests in a vacuum chamber. After further analysis of both the ROSA data, station cameras, and the SPDM inflight joint torque data, it was hypothesized that the wing was imparting small amplitude vibrations back into the arm at the same frequency as the forced motion. This hypothesis could not be easily verified because a triaxial accelerator located on the FRAM was damaged and the photogrammetry targets located on the FRAM were hard to observe. A second observation was that the right edge of the IMBA blanket seemed to vibrate at greater amplitude and lower frequency than the left edge. The reason for this asymmetry is still under investigation but it may have been caused by uneven tensioning in the blanket. As a result of this flapping, the expected blanket modes were often divided into right and left modes.

Table 2 Comparison of FEM frequency predictions with experimental results

Per-Accelerometer Decay Analysis Frequency (Hz)	Per-Accelerometer Excitation Analysis Frequency (Hz)	Eigenvalue Realization Algorithm Analysis Frequency (Hz)	ANSYS Predicted Frequency (Hz)	Abaqus Predicted Frequency (Hz)	Approximate Mode Shape from ERA
0.41	0.40	0.40	0.54	0.50	Structural bending
0.62	0.62	0.61	0.66	0.64	Blanket right edge w/ torsion
		0.68			Blanket right edge w/ torsion
0.82	0.81	0.81			Blanket left edge and center
0.91	0.91	0.91	0.94	0.98	Blanket drum/saddle
1.21	1.20	1.17	0.93		Blanket drum/saddle
1.71	1.70				
1.80	1.80	1.76			Blanket right edge

Blank spaces are modes not predicted or reconstructed by that method

Table 3 Comparison of damping estimates from different methods

Per-Accelerometer Decay Analysis Frequency (Hz)	Per-Accelerometer Decay Analysis Mean Damping (%)	Eigenvalue Realization Algorithm Analysis Frequency (Hz)	Eigenvalue Realization Algorithm Analysis Average Damping Range (%)	Mode Shape from ERA
0.41	2.5	0.40	4.5	Structural bending
0.62	6.1	0.61	1.7	Blanket right edge w/ torsion
		0.68	1.6	Blanket right edge w/ torsion
0.82	0.7	0.81	2.7	Blanket left edge and center
0.91	1.1	0.91	0.6	Blanket drum/saddle
1.21	1.0	1.17	2.1	Blanket drum/saddle
1.71	0.7			
1.80	0.5	1.76	1.6	Blanket right edge

Blank spaces are modes not predicted or reconstructed by that method

Overall, the dynamics of ROSA were consistent throughout four and a half days of testing and over 200 orbits. During cold, nighttime testing, some structural frequencies of vibration increased by 2.5% to 4.5% as shown in Table 4. Other modes were only detectable during daytime or nighttime. Notably, the structure of the solar array wing did not respond in any detectible amplitude during eclipse entry and exit while small high-frequency vibrations were seen in accelerometers on the IMBA over several minutes as the wing emerged from eclipse. This relatively stable response was expected because the carbon composite slit tube booms have a low coefficient of thermal expansion.

Table 4 Day/night shifts in frequencies in ERA results

Mode	Average Daylight Frequency (Hz)	Average Night Frequency (Hz)	Difference (%)	Shape
2	0.60	0.62	3.3	Structural torsion
3	0.67	0.70	4.5	Blanket right edge w/ torsion
4	0.80	0.82	2.5	Blanket left edge and center

With only six accelerometer channels available on the vibrating part of ROSA, it was difficult to discern the shapes of the structural modes numerically. In particular, any mode shape with nodes around the centerline of the blanket could not be detected easily. For this reason, photogrammetry methods were used on video obtained during key

experimental runs in which lighting was favorable to generate displacement data for targets throughout the solar array. This data was used to verify the results described above and to add detail to the rough descriptions of the mode shapes shown in Table 2 and Table 3. The analysis of this photogrammetry data and the results obtained are discussed in the next section.

VI. Photogrammetry Analysis and Results

After the conclusion of the ROSA flight experiment, videos of key experimental runs were downloaded and post-processed using two different approaches [11] by teams at NASA Langley Research Center (LaRC) and NASA Johnson Spaceflight Center (JSC). The post-processing codes used by each team enhanced the visibility of the targets and calculate their positions in each camera's two-dimensional view. Using those positions, three dimensional locations of each target for each video frame were calculated using each approach. By necessity, this analytical effort was somewhat limited. Only four experimental runs were selected for analysis and only a subset of available targets were tracked because both photogrammetry methods were extremely labor-intensive. Only IMBA photogrammetry targets could be analyzed due to difficulty resolving them on the composite booms, mandrel, and FRAM. Finally, quantitative comparisons of the mode shapes is difficult because of the limited number of accelerometers and the fact that there were no photogrammetry targets placed at the same locations as the accelerometers. For this reason, most of the discussion of photogrammetry results in this paper beyond frequency values is limited to qualitative descriptions of shapes and behaviors.

The experimental runs were selected for photogrammetry analysis based on whether they had large responses near modes of interest below 2 Hz, whether they helped to gain complete coverage of the modes in the range of interest, and whether blanket modes were shifting between day and night. The four experimental runs chosen based on these criteria are listed in Table 5. Run 5026 was chosen for very high amplitude responses in the IMBA at several frequencies while run 5074 was chosen both for large responses and an opportunity to see whether the 0.9 Hz daylight mode was really shifting at night. One higher frequency run (5074) was chosen for having several particularly large responses. Finally, the daylight run that excited the largest response around the first structural mode (5080) was chosen for analysis. All four runs were processed by the LaRC team while only runs 5026 and 5074 were processed by the JSC team due to time constraints.

Table 5 Experimental Runs Selected for Photogrammetry Analysis

Run Number	Lighting	Start Frequency (Hz)	End Frequency (Hz)	Duration (s)	Rational for Selection	Processed by JSC?	Processed by LaRC?
5026	Day	0.50	1.25	300	• High right blanket response at ~ 0.6 Hz • High right blanket response at ~ 0.65 Hz • High center blanket response at ~ 0.9 Hz	✓	✓
5052	Night	0.50	1.25	300	• High left blanket response at ~ 0.82 Hz • High center blanket response at ~ 1.16 Hz • Is 1.16 Hz mode a shifted day mode?		✓
5074	Day	1.50	2.00	300	• High right blanket response at ~ 1.68 Hz • High center blanket response at ~ 1.84 Hz	✓	✓
5080	Day	0.37	0.41	180	• High mandrel response at ~ 0.39 Hz		✓

The two photogrammetry analyses were carried out on different subsets of the IMBA targets seen in different lighting conditions in Fig. 6. The LaRC team attempted to track all the IMBA targets but lighting changes cause the algorithms to sometimes lose certain targets. For this reason, the number of targets for which data was generated by the LaRC team ranges from 28 during nighttime run number 5052 to as many as 71 during daytime run number 5026. The JSC team tracked the same select subset of 20 targets during all runs. These targets were selected to give a more comprehensive picture of the response all over the IMBA and to verify the data gathered previously using accelerometers. Since no photogrammetry targets were placed exactly on the locations of the accelerometers, points evenly spaced on either side of them were tracked as analogs. Both sets of displacement time histories generated based on photogrammetry by the two teams were recorded at 30 Hz.

(a) Daylight (b) Eclipse

Fig. 6 ROSA blanket targets and numbering in different lighting conditions

The photogrammetry analyses described in Ref. [11] processed individual frames of various views of the selected experimental runs in order to generate location time histories for each traceable target at a sampling rate of 30 Hz. These time histories were recalculated based on their initial value, meaning that all further analysis discussed here was really conducted on displacements. Some linear time-dependent translations were also removed from the histories of certain targets because the solar array wing was always held in place relative to the stationary cameras. The whole photogrammetry post-processing procedure is shown in Fig. 7.

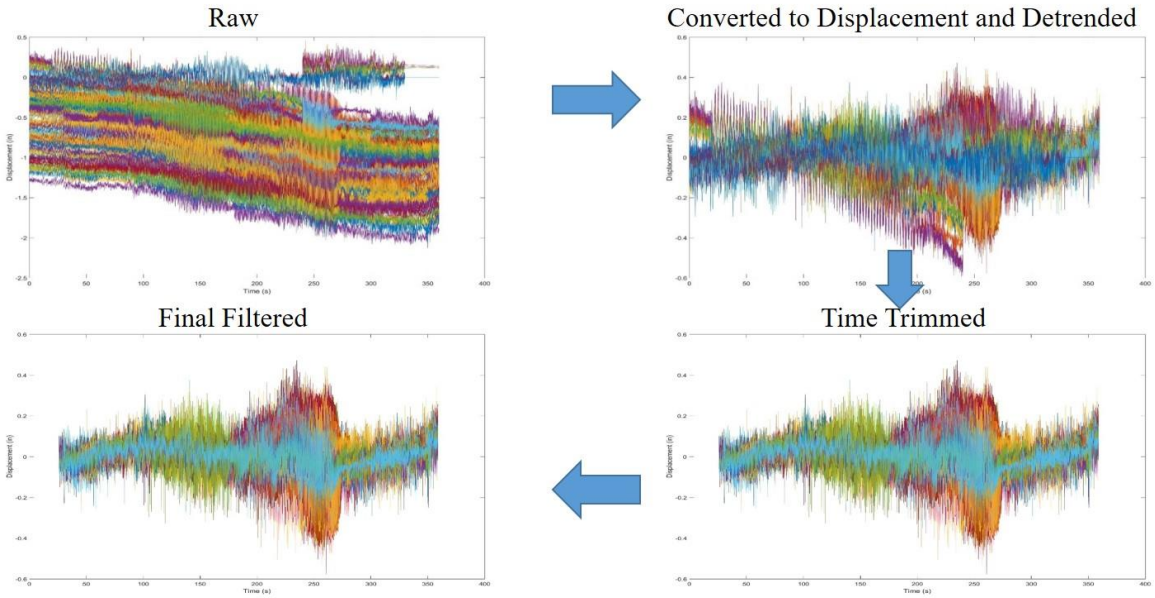

Fig. 7 Post-Processing Procedure Used with Photogrammetry Location Time Histories

The resulting time histories of photogrammetry targets on the IMBA were analyzed in three ways. First, the frequency content for each set of responses was described by calculating a Fast-Fourier Transform (FFT). Second, the Eigenvalue Realization Algorithm was used to identify modes, calculate the damping of the modes, and reconstruct likely mode shapes based on the time histories. Finally, contour plots of significant modes were created by applying a narrow bandpass filter to the data set about the identified mode for a selected target and normalizing the out of plane displacements of all targets to peak displacements of the selected one in a time-consistent manner. The averaged relative displacements were then interpolated over the footprint of the IMBA blanket. Contours were created for both positive and negative peaks. In addition, the Fourier transforms for targets near accelerometer locations were computed, normalized to the maximum peak values and compared to similarly normalized accelerometer data for each run

Significant modes for each target of each run were determined by processing the photogrammetry data through automated scripts. The data was transformed into the frequency domain via FFT and the top 10 modes with peaks >25% of the mean and a minimum distance away from other peaks were collected. These significant modes were

then binned into 0.1Hz bins and counted. Fig. 8 shows the counted modes and spread for each run analyzed as well as a sum over all runs. This plot provides an overview of which modes were active for each run.

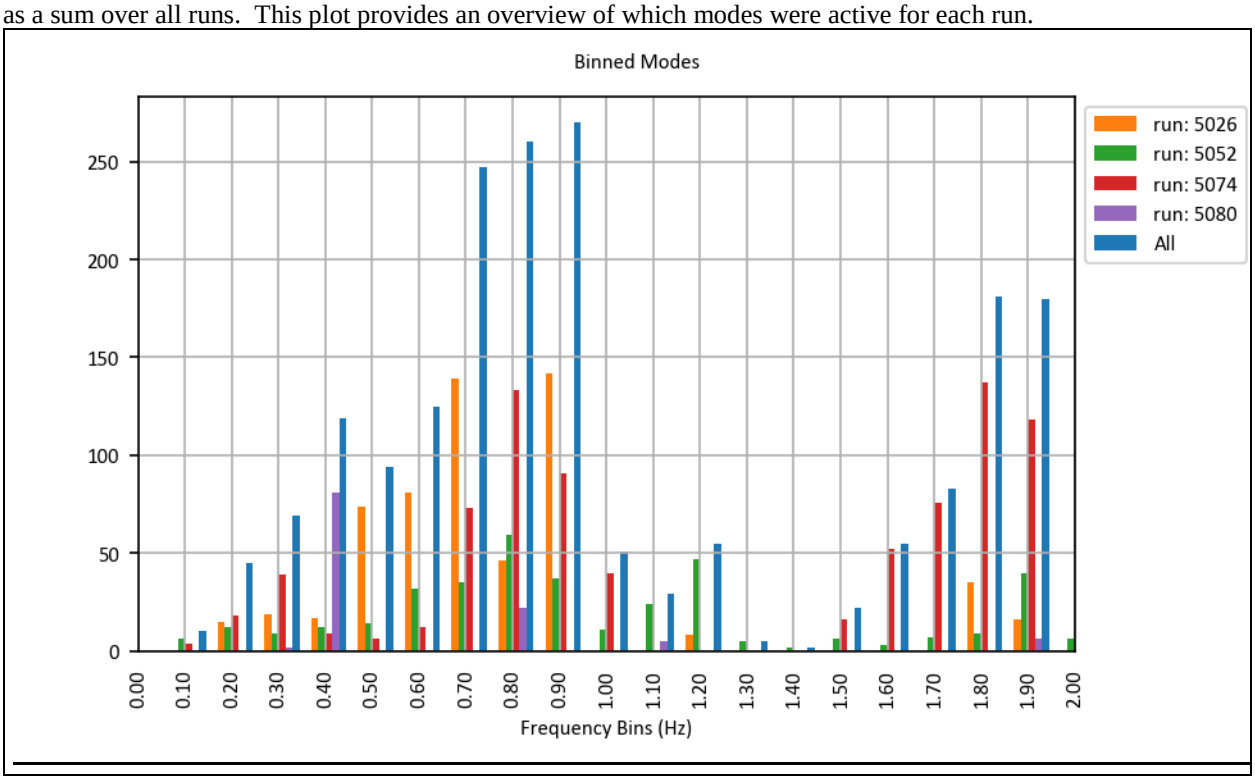

Fig. 8 Significant modes found by automated processing

<u>Analysis of Experimental Run 5080 – Low Frequency Bending</u>

The first experimental run analyzed using photogrammetry data was number 5080, in which a narrow sine sweep between 0.37 and 0.41 Hz was used to excite the first structural bending mode. As shown in FFTs of the six accelerometer time histories and photogrammetry-based displacement time histories for targets near the accelerometers in Fig. 9, the frequencies of the modes detected in this experiment line up quite well with one another at 0.39 Hz. The shape of this mode as reconstructed using ERA on the photogrammetry data is shown in Table 6 along with a contour plot of the normalized out of plane displacements from the point in time at which the mode was measured.

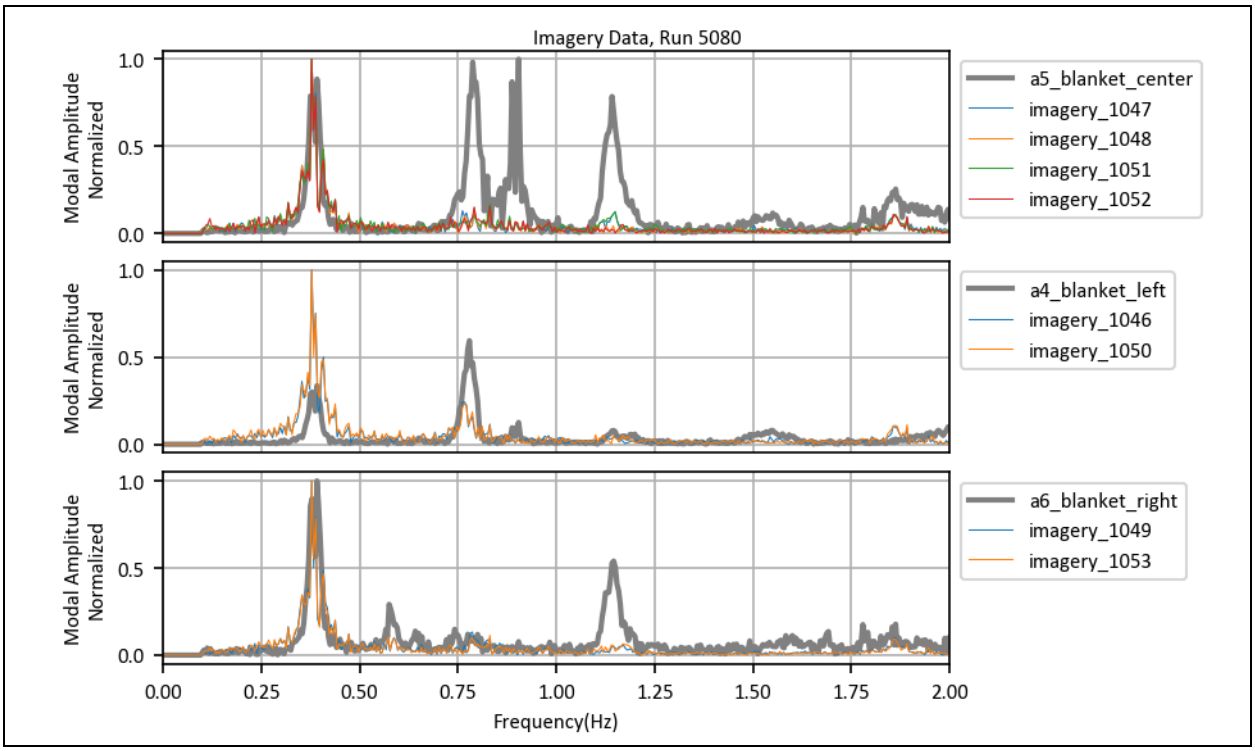

Fig. 9 Comparison of Run 5080 Accelerometer Data with Nearby Photogrammetry Data

Table 6 Modes Identified in Accelerometer and Photogrammetry Data for Run 5080

Frequency [Hz]	Mode Shape Description	Reconstructed Mode Shape and Normalized Deflection Contour
0.39	1st structural bending "diving board"	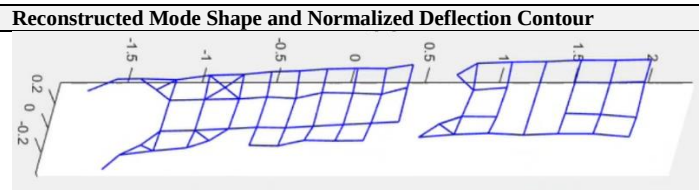
		Normalized Out-of-Plane Deflection Contour 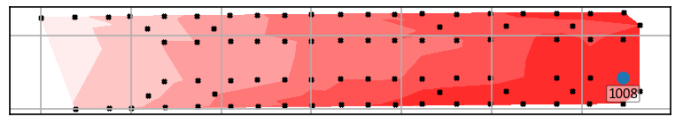

<u>Analysis of Experimental Run 5026 – Low Frequency Daytime Blanket</u>

Experimental run #5026 was analyzed by both the LaRC and JSC photogrammetry teams, resulting in data sets in good agreement with another as seen in the FFT plots in Fig. 10. A few things stand out in these plots, which show FFTs for the accelerometers as well as for the photogrammetry targets in the LaRC and JSC photogrammetry data sets. First, the most prominent structural modes align quite well in all three data sets at around 0.60 Hz, 0.65 Hz, and 0.90 Hz. Second, ERA analysis of both photogrammetry data sets for this run identified a mode at 1.14 Hz. This mode was not seen in the accelerometer data and cannot be seen in the photogrammetry data in Fig. 10 for targets near the accelerometers. Reconstruction of this mode showed it to have characteristics of both the first structural mode and a higher order blanket drum mode. Given its shape and frequency, this may have been another occurrence of the third harmonic of the first structural mode at 0.39 Hz. In addition, a small response is seen at around 1.84 Hz in the photogrammetry data even though it is far outside the range of frequencies intended to be excited in this experiment. This same mode was seen in all photogrammetry data sets, even when the driven frequencies were far lower as seen in Fig. 9.

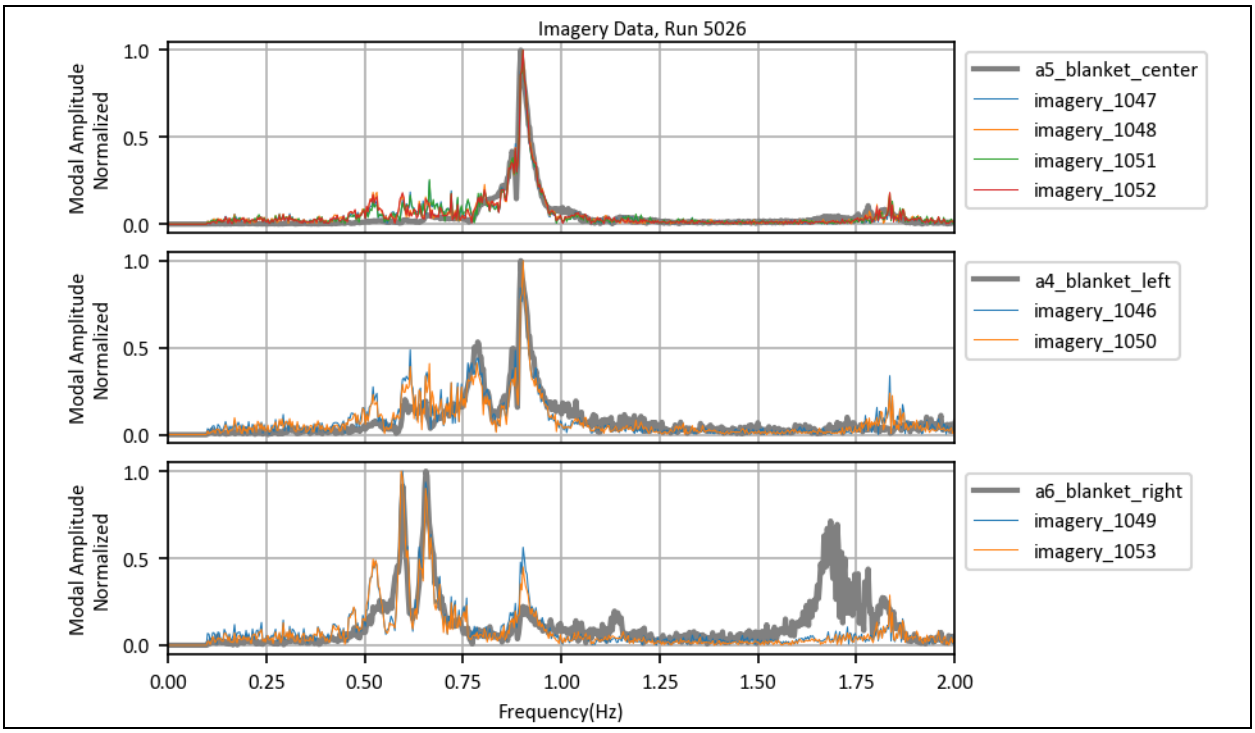

Fig. 10 Comparison of Run 5026 Accelerometer Data with Nearby Photogrammetry Data

Table 7 Modes Identified in Accelerometer and Photogrammetry Data for Run 5026

Frequency [Hz]	Mode Shape Description		
0.61	1st structural torsion and right blanket edge flap	Reconstruction from JSC Data 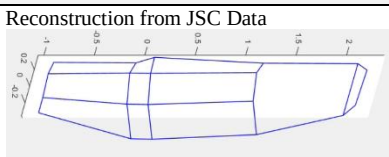	Reconstruction from LaRC Data 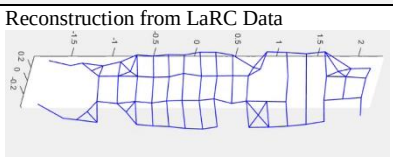
		Normalized Out-of-Plane Deflection Contour 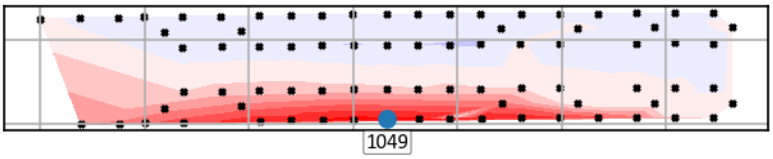	
0.66	1st structural torsion and right blanket edge flap	Reconstruction from JSC Data 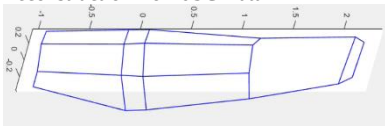	Reconstruction from LaRC Data 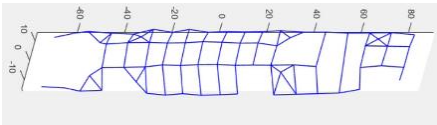
		Normalized Out-of-Plane Deflection Contour 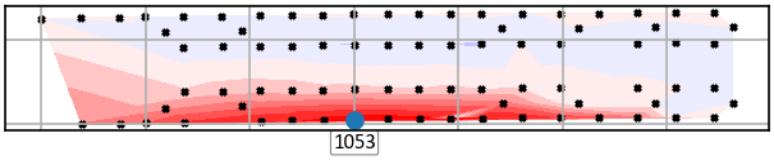	
0.78	Left blanket edge flapping	Reconstruction from JSC Data *No good reconstruction found*	Reconstruction from LaRC Data

			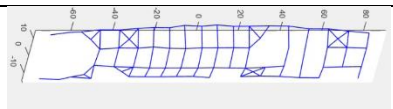
		Normalized Out-of-Plane Deflection Contour 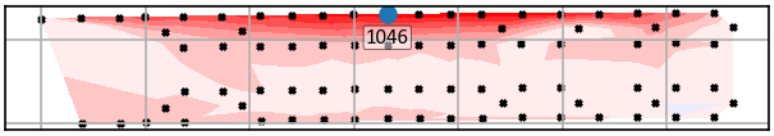	
0.89	1st blanket drum/saddle	Reconstruction from JSC Data 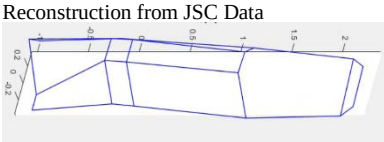	Reconstruction from LaRC Data 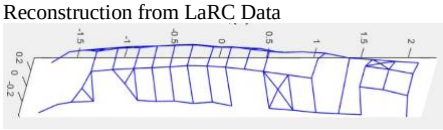
		Normalized Out-of-Plane Deflection Contour 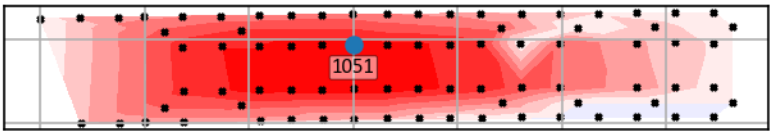	

Where it was possible to generate ERA reconstructions of the modes excited in run 5026, their frequencies and shapes are shown in Table 7. These reconstructions show that previous descriptions of mode shapes based on accelerometer data were largely accurate. The two modes at about 0.61 and 0.66 Hz are very similar, combining structural twist with blanket twist. The 0.78 Hz mode was harder to characterize but on video appears to involve the left edge and center of the blanket flapping similar to the way the right edge flaps at lower frequencies.

Analysis of Experimental Run 5052 – Low Frequency Nighttime Blanket

Run number 5052 was chosen to study what effects night temperatures have on the low frequency blanket modes. The frequency content of the photogrammetry data shown in Fig. 11 matches up very well with that of the accelerometer data but, as shown in Table 8, each blanket mode has shifted slightly higher by as much as 9%. An assumption must be made that these are the same blanket modes because the lighting at night limited the number of targets available for tracking and made comparison of the mode shapes difficult. This also makes it harder to reconstruct mode shapes using ERA except the mode at 1.17 Hz. This mode shape is hard to discern as a static figure but when animated looks very similar to the 0.89 Hz blanket saddle/drum mode found during daylight run number 5026, lending further credence to the observation made previously [10] that this mode may be shifting by about 33% between day and night.

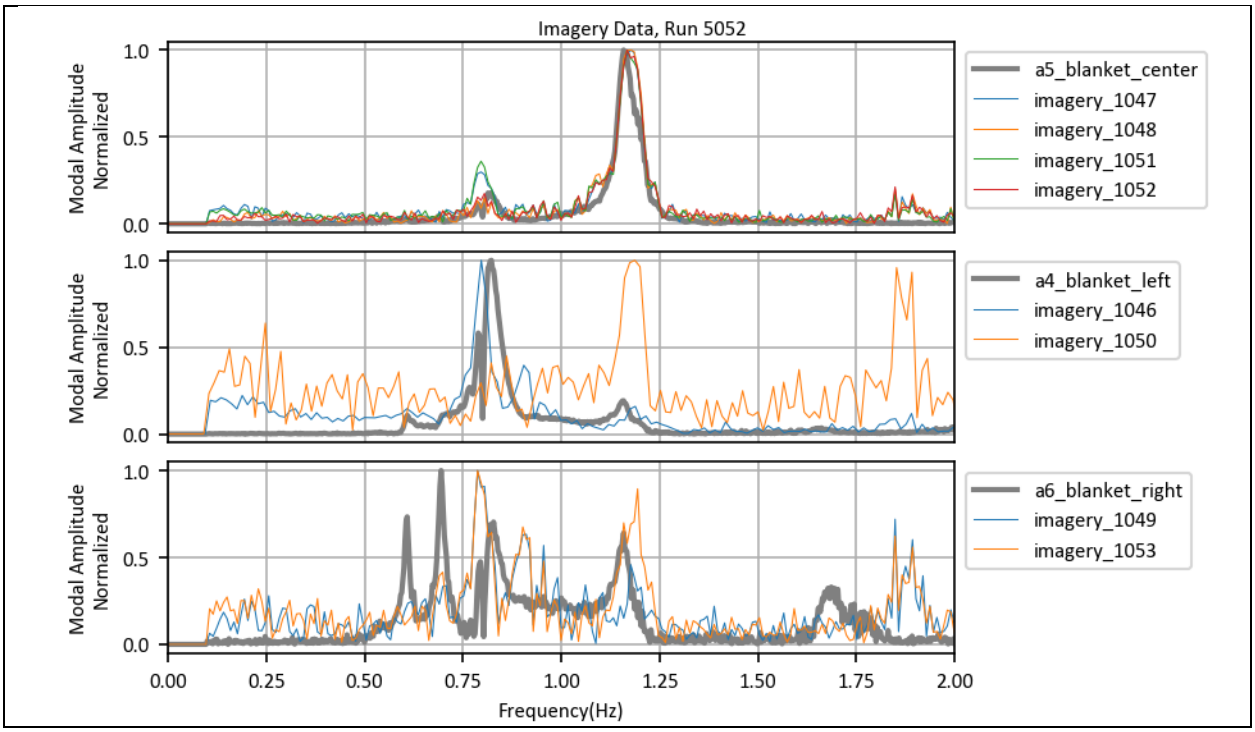

Fig. 11 Comparison of Run 5052 Accelerometer Data with Nearby LaRC Photogrammetry Data

Table 8 Modes Identified in Accelerometer and Photogrammetry Data for Run 5052

Frequency [Hz]	Mode Shape Description	Reconstruction from LaRC Photogrammetry Data
0.61	1st structural torsion and right blanket edge flap	*No good reconstruction found*
0.69	1st structural torsion and right blanket edge flap	*No good reconstruction found*
0.82	Left blanket edge flapping	*No good reconstruction found*
0.95	1st blanket drum/saddle	*No good reconstruction found*
1.17	1st blanket drum/saddle	Reconstruction from LaRC Data 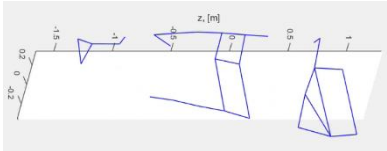 Normalized Out-of-Plane Deflection Contour 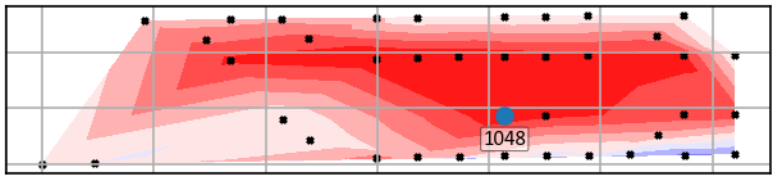

Analysis of Experimental Run 5074 – High Frequency Daytime Blanket

Experimental run number 5074 exhibited the highest blanket accelerometer responses for two modes of interest in the high range of the excited frequencies. As seen in Fig. 12, the relatively low and closely-spaced accelerometer responses suggested jumbled, perhaps combined modes but the photogrammetry data from both sources show clear responses at two distinct frequencies around 1.64 Hz and 1.83 Hz respectively. It is also interesting to note that the 1.83 Hz mode shows up clearly in photogrammetry data for all the runs examined in this paper, something that cannot be said of the accelerometer data. This phenomena is likely explained by the two reconstructed mode shapes shown in Table 9. Both of the modes excited in this experiment have nodes at the center of the blanket for at least two of the accelerometers located there, meaning they would register very little response. Photogrammetry, with its ability to gather throughout the IMBA, was better able to pick up these modes and describe them.

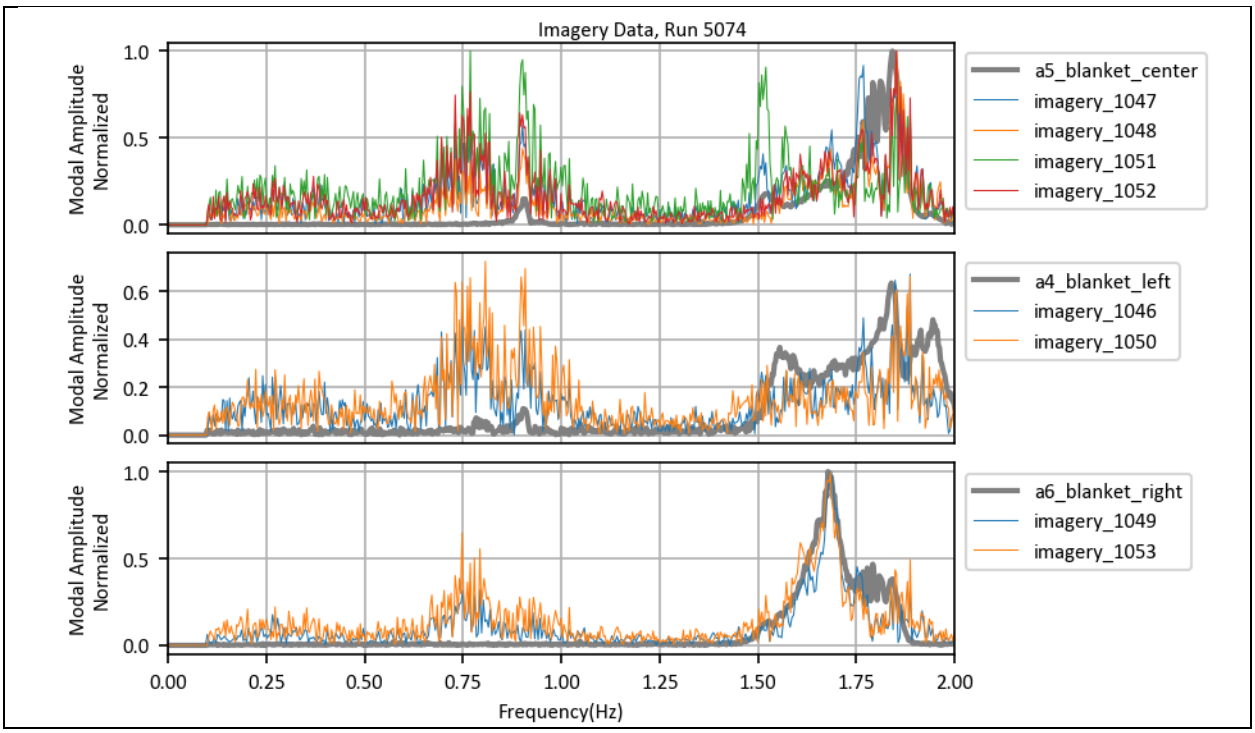

Fig. 12 Comparison of Run 5074 Accelerometer and Photogrammetry Data

Table 9 Modes Identified in Accelerometer and Photogrammetry Data for Run 5074

Frequency [Hz]	**Mode Shape Description**	Reconstruction from JSC Photogrammetry Data	Reconstruction from LaRC Photogrammetry Data
1.64	3rd order right blanket edge flap	Reconstruction from JSC Data 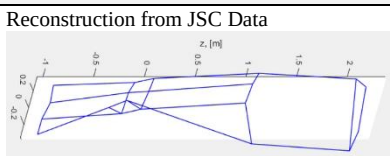	Reconstruction from LaRC Data 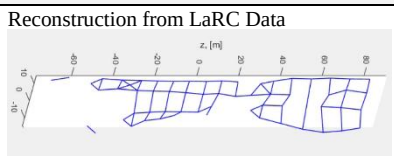
		Normalized Out-of-Plane Deflection Contour 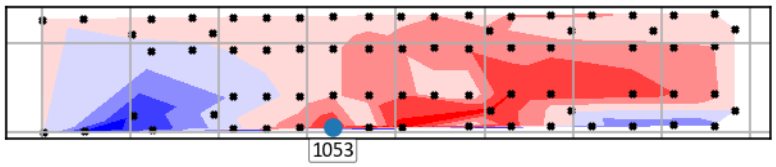	

1.83	2nd order blanket drum/saddle	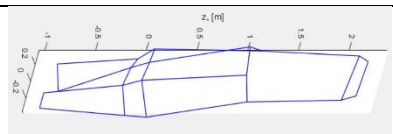	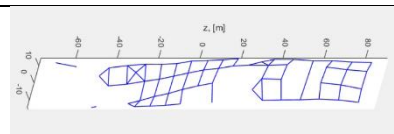
		Normalized Out-of-Plane Deflection Contour 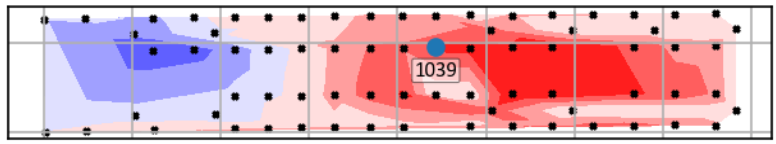	

VII. Discussion

Ongoing analysis of the ROSA flight experiment on the International Space Station has allowed us to learn more about the details of its structural dynamics and changes in its behavior between day and night. In previous work [10], data from accelerometers was used to identify a group of 8 structural modes below 2 Hz but details of the shapes associated with those modes could only be acquired through visual inspection of video. In this paper, photogrammetry data gleaned from video from four experimental runs was carefully analyzed to verify previous conclusions and to give a more complete picture of each of the eight modes. These modes are shown with average measured frequencies and damping (measured only with accelerometers) in Table 10. This analysis proved to be very successful, especially for the tensioned blanket modes. The results in terms of the frequencies measured are remarkably consistent with accelerometer data.

Table 10 Summary of Structural Modes of ROSA

System Mode	Based on Accelerometer Data		Based on Photogrammetry Data		Damping [%]
	Frequency [Hz]	Previously Assumed Mode Shape	Frequency [Hz]	Confirmed Mode Shape	
1	0.41	1st structural bending	0.39	1st structural bending "diving board"	3.50
2	0.60	Blanket right edge w/ torsion	0.61	1st structural torsion and right blanket edge flap	3.90
3	0.66	Blanket right edge w/ torsion	0.66	1st structural torsion and right blanket edge flap	1.60
4	0.81	Blanket left edge and center	0.78	Left blanket edge flapping	1.70
5	0.91 *	Blanket drum/saddle (day)	0.89 *	1st blanket drum/saddle (day)	0.85
6	1.18 *	Blanket drum/saddle (night)	1.14 *	1st blanket drum/saddle (night)	1.55
7	1.71	Blanket right edge	1.64	3rd order right blanket edge flap	0.70
8	1.80	Blanket right edge	1.83	2nd order blanket drum/saddle	1.05

Two important observations in previous work [10] were backed up by the results generated here. The first structural mode was about 20 % lower than expected prior to flight. It is suspected that similarities between the first structural modes of the ROSA flight experiment and the ISS robot arm created a coupled structure with a lower fundamental frequency than expected, however this has been hard to prove numerically because the tri-axial accelerometer on the base of ROSA was broken and photogrammetry algorithms failed to pick up targets on the base. The asymmetry in the blanket modes starting with the flapping right edge mode around 0.61 Hz was also confirmed here and shown to likely have coupled with the predicted structural twist mode at about the same frequency.

The photogrammetry data proved especially valuable in this experiment because of the limited amount of instrumentation that could be placed on ROSA. Although the single set of three accelerometers on the solar array could characterize the first modes of the structure and blanket, higher order modes were harder to measure. In particular, the value of the photogrammetry is shown in the 1.83 Hz mode whose nodes are coincident with the accelerometer locations, making detection by that means difficult. Further investigation of photogrammetry data at higher frequencies would probably reveal and describe even more blanket modes like this one.

The experimental runs analyzed here seem to back up the observation made previously that IMBA blanket modes are slightly higher at night during cold temperatures than when exposed to sunlight. While most of the blanket modes only shift by a few percentages between day and night, the blanket saddle/drum mode measured at about 0.90 Hz during the daytime runs looks very similar to a mode that has a frequency roughly 33% higher at night. The root cause of these shifts is unexplained at this time.

All in all, the structural dynamics of ROSA and its lightweight solar array blanket have been well characterized but there remains a great deal of data that could provide further insight into some of the interesting behaviors discussed here. Only four experimental runs were analyzed in this paper out of dozens for which video exists. Further analysis

of other runs would be useful for verifying the observations made here. Similarly, it could be beneficial to renew efforts to track the targets on the structure of ROSA and the FRAM. Should future photogrammetry techniques make it possible to track the structure, a more comprehensive numerical comparison between accelerometer and photogrammetry data would be possible. The ability to track of targets on the FRAM would allow exploration of the theorized structural interaction between ROSA and the ISS robot arm and perhaps a more accurate measurement of ROSA's independent first structural bending mode.

VIII. Acknowledgments

This flight experiment has required the tireless effort and unwavering support of dozens of individuals and organizations. The Air Force Research Laboratory Space Vehicles Directorate provides principle experiment design, oversight, and sponsorship. Launch was brokered by and payload integration was funded and managed by the Department of Defense (DoD) Space Test Program (STP) Houston office. The Space Test Program developed the jettison system and the robotic interfaces to the OTCM. They also led the integration of the completed payload to the ISS and to the SpaceX Dragon capsule in addition to developing the command and data handling architecture needed to get from the payload to the ground, and commands from the ground to the payload. ROSA hardware design, development, construction, and testing was provided by Deployable Space Systems, Inc. Ecliptic Enterprises Corp. developed the data acquisition and control unit. LoadPath, LLC., in conjunction with AFRL fabricated and validated the composite slit tube columns and material system. Photogrammetry metrology system design and analysis was provided by the NASA Langley Research Center (LaRC) Advanced Measurements and Data Systems Branch and the Johnson Space Center (JSC) Image Science and Analysis Group. The LaRC Structural Dynamics Branch assisted with structural dynamics analysis predictions. Additional mission funding was provided by the U.S. Air Force Space and Missile Systems Center (SMC/AD).

IX. References

[1] Banik, J.A., and Hausgen, P., " Roll-Out Solar Arrays (ROSA): Next Generation Flexible Solar Array Technology for DoD Spacecraft," *2017 AIAA SPACE and Astronautics Forum and Exposition*, 12-14 September 2017, Orlando, Florida. AIAA-2017-5307.

[2] Banik, J., Urioste, B., "Chapter 7: Spaceflight Testing," *Testing Large Ultra-Lightweight Spacecraft. AIAA Progress Series in Aeronautics and Astronautics*. Vol 253. 2017. pp. 215-253.

[3] Banik, J., LaPointe, M., Kiefer, S., "On-Orbit Validation of the Roll-Out Solar Array," *IEEE Aerospace 2018 in Big Sky, MT*, 4-11 March 2018. Accepted for Publication.

[4] ASA homepage, International Space Station Research and Technology, Roll Out Solar Array (ROSA) https://www.nasa.gov/mission_pages/station/research/experiments/2139.html Accessed 15 April 2017.

[5] Werner, D., "Market Disruptor", *Aerospace America*, October, pp. 34-38, 2017.

[6] Genna, M., "Innovation: Solar Array Success for SSL Implementation—A Space Systems Loral Focus", *SatMagazine*, September, pp. 104-105, 2017.

[7] Banik, J.A., Kiefer, S.H., LaPointe, M. and P. LaCorte, "On-Orbit validation of the Roll-Out Solar Array," *39th IEEE Aerospace Conference*, 3-10 March 2018, Big Sky, MT.

[8] Spence, B., LaPointe, M., White, S., LaCorte, P., and S. Kiefer, "International Space Station (ISS) ROSA Solar Array Flight Experiment Mission and Results," *36th Annual Space Power Workshop*, 23-25 April 2018, Los Angeles.

[9] Yates, H. and B. Hoang, "SSL ROSA Qualification Status," *36th Annual Space Power Workshop*, 23-25 April 2018, Los Angeles.

[10] Chamberlain, M.K., Kiefer, S.H., and Banik, J.A., "On-Orbit Structural Dynamics Performance of the Roll-Out Solar Array," *4th AIAA Spacecraft Structures Conference, AIAA SciTech Forum*, 8-12 January 2018, Orlando, FL. AIAA-2018-1942.

[11] Jones, T.J., Liddle, D.A., Shortis, M.R., and J.A. Banik, "On-Orbit Photogrammetry Analysis of the Roll-Out Solar Array (ROSA), accepted for the *6th AIAA Spacecraft Structures Conference, AIAA SciTech Forum*, 7-11 January 2019, San Diego, CA.

[12] Chamberlain, M.K., Kiefer, S.H., and Banik, J.A., "Structural Analysis Methods for the Roll-Out Solar Array Flight Experiment", accepted for the *6th AIAA Spacecraft Structures Conference, AIAA SciTech Forum*, 7-11 January 2019, San Diego, CA.

[13] Juang, J.-N., Horta, L.G., and Phan, M.: "System/Observer/Controller Identification Toolbox from Input/Output Measurement Data." User's Guide, NASA TM-107566, 1992.

[14] Horta, L.G., Juang, J-N, and Chen, C.-W.: "Frequency Domain Identification Toolbox." NASA TM-109039, 1996.